Experimental Research and Numerical Analysis on Sloshing Dynamics of Irregular Annular Cylindrical Water Tank

Xiaojun Li, Chenning Song, Guoliang Zhou, Chao Wei, Ming Lu

***Abstract*—**This study focuses on the irregular annular cylindrical water tank of nuclear island building. Water tank is one important component of passive containment cooling system (PCS). The sloshing frequency of water is much less than the structure frequency and large-amplitude sloshing occurs easily subjected to seismic loadings. It is known that the floor response spectra may be changed because of the water tank and so do the seismic response of nuclear equipment. Therefore, the sloshing dynamics of water tank should be studied before the dynamic analysis of nuclear island building. A 1/16 scaled model was designed, and the shaking table test was done. The hydrodynamic pressure time histories and variation in wave height were recorded in the test. Then, the sloshing frequencies and damping ratio are recognized. Moreover, modal analysis and time history analysis of numerical model were done based on ADINA. By comparing the sloshing frequencies and hydrodynamic pressures, the reasonableness of test method and the accuracy of numerical results are verified, and it indicates that the formulation of potential-based fluid elements (PBFE) can be used to simulate fluid-structure interaction (FSI) of nuclear island building.

***Keywords*—**Nuclear island building, water tank, sloshing dynamics, shaking table experiment, PBFE.

I. Introduction

PCS system is the significant characteristic of the third-generation nuclear power plants [1], which is different from the traditional nuclear power plants. As known that the sloshing frequency of water is far less than structure frequency, so the long period components of seismic loadings could not be ignored in the analysis of water tank. Moreover, the influence of water tank on floor response spectra under seismic loadings should be considered emphatically. The dynamic characteristics of water tank should be studied to analyze the seismic response of nuclear island building accurately.

In the research on water tank of nuclear power plants, Zhao et al. [2]-[4] used the Arbitrary Lagrange Eulerian (ALE) algorithm to simulate the seismic response of AP1000 shield building and studied the influence of water tank. The research showed that water tank could reduce the dynamic response of structure. Xu et al. [5] used the smoothed particle hydrodynamics (SPH) and finite element method (FEM) coupling method to simulate the FSI. The research showed that the water tank could decrease the natural frequency and response of the shield building. Lu et al. [6] built a scaled elevated tank to investigate the seismic response of shield building under transient loadings. Moreover, numerical models were established and the numerical results of acceleration and displacement were in good agreement with the experiment. Liu et al. [7] did the shaking table test of a scaled elevated tank of passive containment cooling system water storage tank (PCCWST). An equivalent mechanical model was used to predict the seismic forces of the PCCWST subjected to horizontal ground excitation and the numerical results had a good agreement with the experiment. Zeng et al. [8] designed a 1/40 scaled model of elevated water tank and did the shaking table test. The experimental results verified the feasibility of calculation method about sloshing impact force proposed by Lu [9].

In the research on dynamic characteristics of water tank, the main test method is using laser displacement sensor to measure the sloshing displacement of water, then the sloshing frequency could be calculated. Wang et al. [10] measured the time-histories of wave height by laser displacement sensor and obtained the sloshing frequency and damping ratio. Takahara and Kimura [11] studied the frequency response of the annular cylindrical water tank subjected to pitching excitation. By comparing the theoretical analysis and test results, the importance of non-linear analysis was verified to evaluate the sloshing response. Wang and Lu [12] developed a sloshing simulation system for vessel tanks and used the laser displacement sensor to record the motion situation of water under external excitation. Li et al. [13] used the scan laser measure instrument to collect the velocity response of water surface. Then, the sloshing frequency and fluctuation could be got by the fast Fourier transformation (FFT) of velocity time-histories. Aimed at sloshing damping ratio, the analytical solution or approximate solution was derived only for containers with regular shape. The dynamic experiment was the common used method to obtain sloshing damping ratio, but the

X. J. Li is with the Institute of Geophysics, China Earthquake Administration, China, Beijing, 100081 China, and also College of Architecture and Civil Engineering, Beijing University of Technology, Beijing, 100124 China (e-mail: beerli@vip.sina.com).

C. Song is with the College of Architecture and Civil Engineering, Beijing University of Technology, Beijing, 100124 China (corresponding author, phone: +8613801384356; e-mail: scanner2007@163.com).

G. L. Zhou is with the Nuclear and Radiation Safety Center, Ministry of Environmental Protection of the People's Republic of China, Beijing, 100082 China (corresponding author, phone: +8613520794365; e-mail: zgl_iem@163.com).

C. Wei is with the Nuclear and Radiation Safety Center, Ministry of Environmental Protection of the People's Republic of China, Beijing, 100082 China (e-mail: zgl_iem@163.com).

M. Lu is with the Institute of Crustal Dynamics, China Earthquake Administration, Beijing, 100085 China (e-mail: luming6@yeah.net).

experimental results were lack of repeatability because of the non-linear characteristic.

Sloshing frequency and damping ratio are the key parameters of dynamic characteristic. Moreover, they are also the key parameters to simplify the sloshing analysis based on Housner model. Related scholars have done some research on the sloshing frequency [14]-[16] and specifications [17]-[19] also give the simplified calculation formulas on regular cylindrical tanks. But, for irregular annular cylindrical water tank, related specifications do not give detailed introduction. Aimed at sloshing damping ratio, suggested values have been given for regular containers, but for irregular containers, the research and verification are deficient.

In this study, a 1/16 scaled model was made for shaking table test. Pore water pressure sensors (PWPS) were arranged along the different height of tank walls, and the cameras were arranged on the top of the tank to record the hydrodynamic pressure time-histories and attenuation data of wave height. The sloshing frequency and damping ratio can be obtained based on the test data. By comparing the experimental results and numerical analysis, the reasonableness of experimental method and the accuracy of numerical are verified.

II. Shaking Table Test

A. Introduction of Model

The experimental model was designed with a geometrical scale of 1/16. To satisfy the rigid assumption of water tank, the tank walls and bottom were made using microconcrete and the steel bars were replaced by galvanized iron wires. To test the wave height, the roof of water tank was replaced by toughened glass and connected to the water tank with fixed parts. The experimental model and the geometry sizes are shown in Fig. 1.

To study the sloshing characteristic of liquid, the existing test instruments are often laser displacement sensor or laser vibration measuring instrument. Common laser displacement sensor might not satisfy the testing precision, but the high precision instruments or collection systems are very expensive. According to the theory of laser measurement, colored substance dissolved by organic solvent is used to increase laser reflection. However, organic solvent like lacquer thinner is easily volatile and may bring some risks. Moreover, this method could not catch the splash liquid during the test, and the organic solvent may change the sloshing characteristic of liquid itself. Therefore, to recognize the sloshing frequency and damping ratio, PWPS shown in Fig. 2 were used to measure the hydrodynamic pressure in this paper.

To record the hydrodynamic pressure data, 16 PWPS were divided into two groups and they were arranged along the height of tank walls in X cross section and Y cross section separately. To record the attenuation data of wave height, rulers are arranged at the tank walls in X cross section and Y cross section. In addition, cameras were arranged on the top of toughened glass. The arrangements of PWPS and cameras are shown in Fig. 3. The material parameters of experimental model are listed in Table I.

(a)

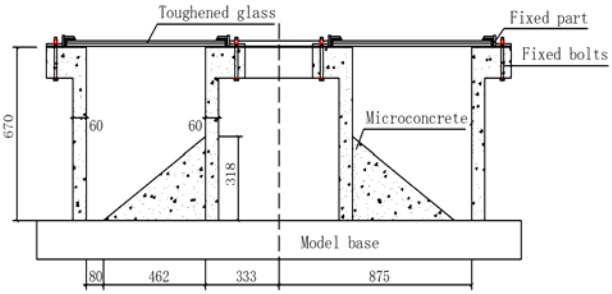

(b)

Fig. 1 Introduction of model (a) Experimental model, (b) The profile and geometry sizes

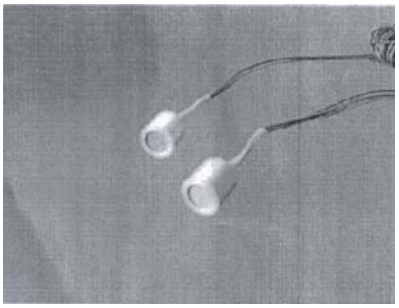

Fig. 2 Pore water pressure sensors (PWPS)

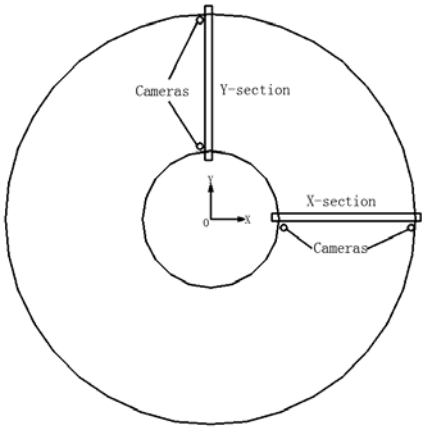

(a)

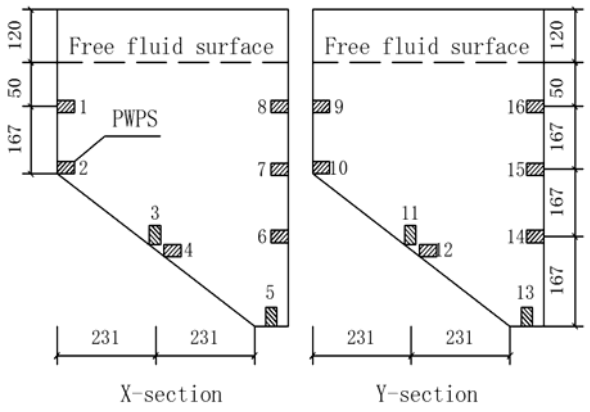

(b)

Fig. 3 Layout of instruments (a) Top view of model, (b) Layout of PWPS

TABLE I
MATERIAL PARAMETERS OF EXPERIMENTAL MODELS

	Microconcrete	Toughened glass	Galvanized iron wires	Water
Material parameters				
density (kg/m^3)	2350	2560	7800	1000
Young' modulus (Pa)	1.05×10^{10}	7.20×10^{10}	2.06×10^{11}	—
bulk modulus (Pa)	—	—	—	2.30×10^{9}
poisson' ratio	0.17	0.20	0.30	—

B. Experiment Process

According to the geometrical scale of 1/16, the height of free water surface is 550 mm. To recognize the sloshing frequencies, single-direction sine waves were used. The normalized sine wave is shown in Fig. 4 (a) and the peak ground accelerations are 0.05 g and 0.10 g. To verify the reasonableness of numerical results, the three-direction acceleration time histories were used as inputs. The time history curves are shown in Fig. 4 (b), and the peak ground accelerations of three-direction time histories are 1.20 g, 0.80 g, and 0.60 g separately. Hydrodynamic pressure and attenuation data of wave height were recorded. Then, the sloshing frequency and damping ratio were obtained.

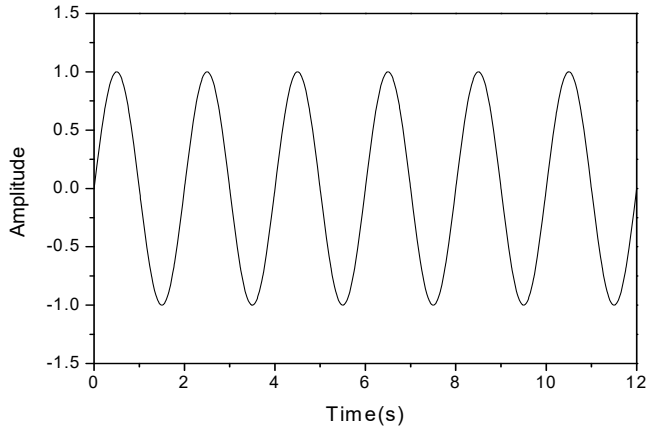

(a)

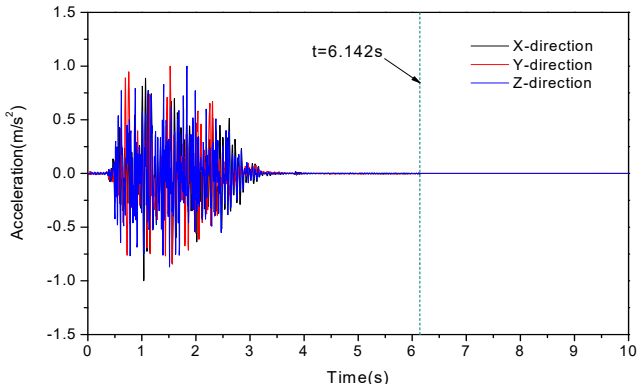

(b)

Fig. 4 Input time history curves for saking table test (a) Normalized sine wave, (b) Normalized seismic inputs in three directions

C. Data Analysis

1. Recognition of Sloshing Frequency

FFT is widely used in the field of physics, acoustic, optics, structure dynamics and signal processing. Based on FFT of data-signal, the sloshing frequency of liquid can be recognized through hydrodynamic pressure. The typical application of FFT is changing time histories into amplitude-frequency curves and the basic equation is shown as follows:

$$F(\omega)=\int_{-\infty}^{+\infty} f(t)e^{-i\omega t}dt \tag{1}$$

where $f(t)$ is the time history of data-signal, $F(\omega)$ is the spectrum function of $f(t)$ and ω is the frequency.

In the experiment, the liquid would keep sloshing and the wave height would gradually decay when the external excitation is ended. At that time, the hydrodynamic pressure and wave height only reflect the dynamic characteristic of liquid in the tank without external excitation. As shown in Fig. 5, hydrodynamic pressure in the free sloshing range was obtained, and the pressure-time curves can be changed into amplitude-frequency curves by FFT. From Fig. 5 (c), the sloshing frequencies can be recognized.

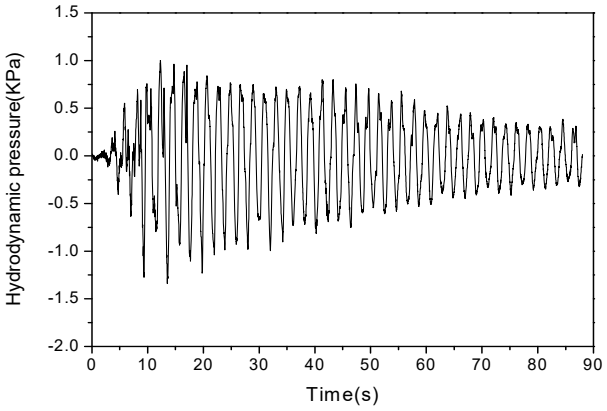

(a)

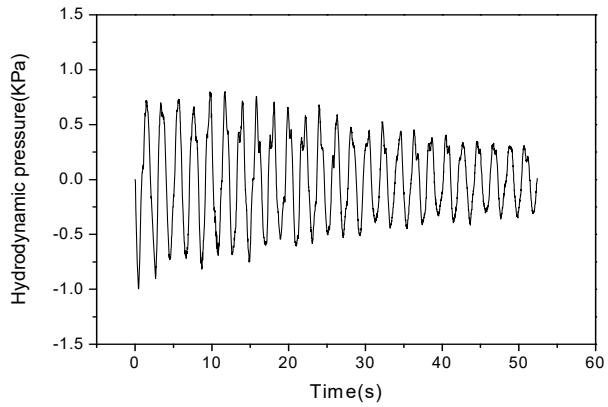

(b)

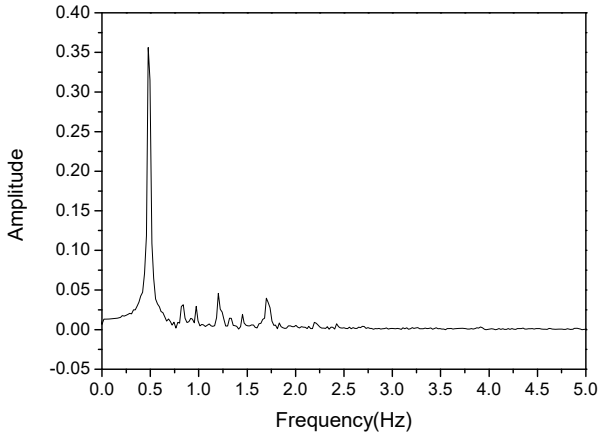

(c)

Fig. 5 Data processing of hydrodynamic pressure records (a) Time history curve, (b) Free sloshing range, (c) Amplitude-frequency curve

Low sloshing frequencies play a control action in the dynamic analysis of liquid and seismic design of containers, especially the 1st sloshing frequency. So, the first few sloshing frequencies are needed to be recognized. The statistical results of first four sloshing frequencies recognized by hydrodynamic pressure data are listed in Table II. Moreover, 40 samples are chosen, and the errors between average value and test value are shown in Fig. 6. As shown in Table II, the coefficients of variation are all less than 5%. In Fig. 6, the maximum errors of first four sloshing frequencies are 3.56%, 5.96%, 5.68%, and 2.91%, separately. It proves that the test values have little discreteness and the results are acceptable.

TABLE II
FIRST FOUR SLOSHING FREQUENCIES

Modes	Average value (AVG) (Hz)	Standard deviation (SD) (Hz)	Coefficient of variation (%)
1	0.4938	0.0090	1.82
2	0.8404	0.0270	3.21
3	1.0015	0.0267	2.67
4	1.2188	0.0194	1.59

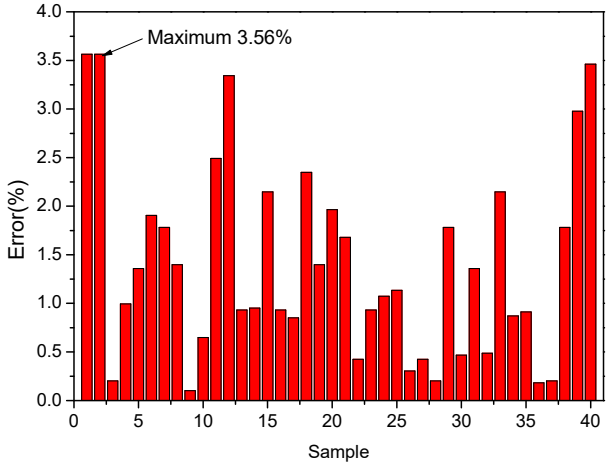

(a)

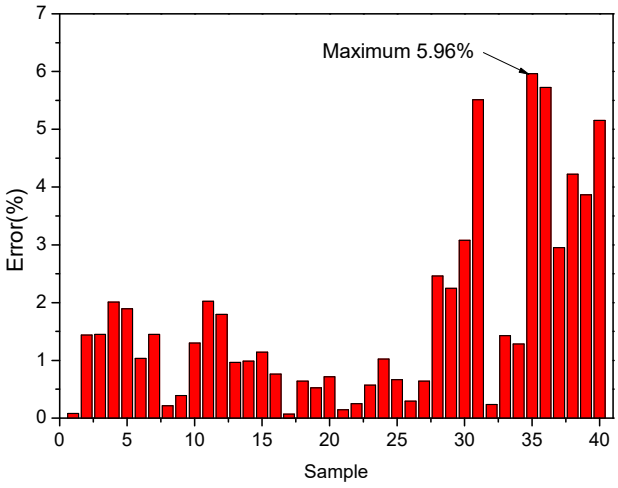

(b)

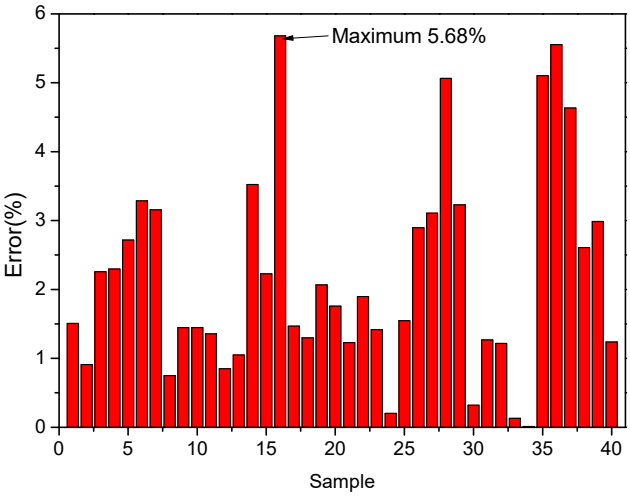

(c)

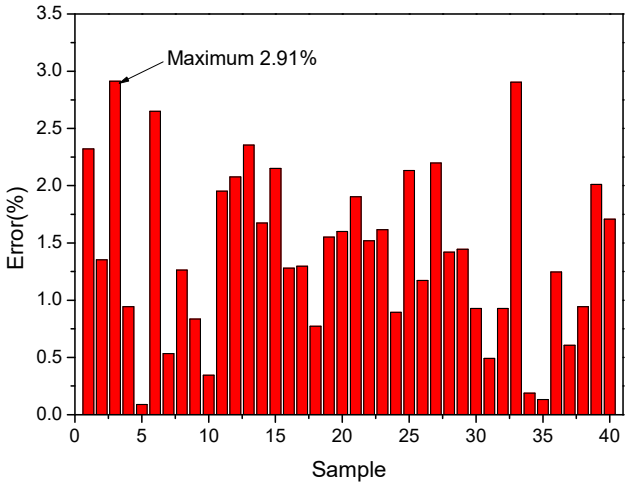

(d)

Fig. 6 Statistics of errors between average value and test value (a) 1st sloshing frequency, (b) 2nd sloshing frequency, (c) 3rd sloshing frequency, (d) 4th sloshing frequency

2. Recognition of Sloshing Damping Ratio

As one important dynamic parameter, sloshing damping is mainly from the friction between liquid and container. The value is related to four factors: viscous damping of inner wall, viscous dissipation of free fluid surface, viscous dissipation of liquid inside and capillary of liquid inside. The sloshing damping ratio is often obtained through experiment because of the complexity of parameters. In this study, the 1st natural frequency of water tank is more than 50 Hz and the model could be regarded as rigid tank. The specifications [18], [19] propose that the sloshing damping ratio is 0.5% for normal tanks. However, it should be noted that for higher viscosity fluids and tanks with internal baffles, the damping ratio is higher. For the impulsive components, the damping ratio is generally assumed to be approximately 2%. For irregular containers, the specification does not give the suggestion.

Logarithmic decrement method is used to calculate the sloshing damping ratio in this paper and the equation is shown:

$$\delta = \ln \frac{\mu_i}{\mu_{i+1}} = \frac{2\pi\xi}{\sqrt{1-\xi^2}} \tag{2}$$

where δ is the logarithmic decrement, μ_i and μ_{i+1} are the amplitudes of two adjacent periods, ξ is the damping ratio.

On account of the small sloshing damping, the free vibration of liquid decays slowly. To satisfy the accuracy requirement, the amplitudes of j adjacent periods are used to calculate the damping ratio. The damping ratio of small damping system can be calculated using equation:

$$\xi \approx \frac{1}{2\pi j} \ln \frac{\mu_i}{\mu_{i+j}} \tag{3}$$

TABLE III
STATISTICS OF SLOSHING DAMPING RATIO

Average value (AVG) (%)	Standard deviation (SD) (%)	Coefficient of variation (%)
0.5138	0.0212	4.13

Based on (3), 40 video samples are chosen to calculate the sloshing damping ratio of water. The results are shown in Table III and Fig. 7. The coefficient of variation is less than 5%, and the discreteness is small. As shown in Fig. 7, the test values are almost between AVG-SD and AVG+SD. It proves that the experimental results are reasonable and reliable. The average value of sloshing damping ratio is 0.5138%, and it has a good agreement with the suggestion in the specifications. Although the container is irregular annular cylindrical water tank, the sloshing damping ratio is insensitive to the shape of tank. The reasons may be that the water tank is rigid and the sloshing damping ratio is small.

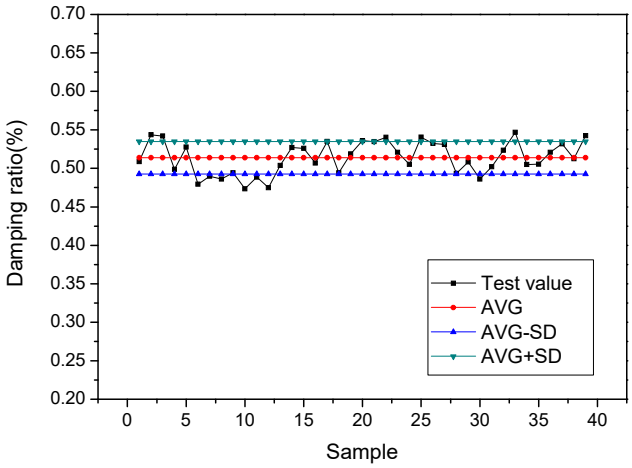

Fig. 7 Statistics of sloshing damping ratio

III. Numerical Analysis and Discussion

A. Description of Numerical Model

In the field of FSI, ADINA software has strong solving capability. The equations of the $\phi - u$ formulation in this study are briefly introduced in this part.

As the special fluid element in ADINA [20], the PBFE can be used for frequency and time-history analyses of structure [21], [22]. There are two basic parameters in the formulation: velocity potential ϕ and displacement u. The velocity potential ϕ satisfies:

$$\nabla^2\phi = \frac{1}{C_w^2}\frac{\partial^2\phi}{\partial^2 t} \tag{4}$$

where ∇^2 is the Laplace differential operator, t is the time variable, C_w is the wave velocity in fluid which is given by

$$C_w = \sqrt{\kappa_w / \rho_w} \tag{5}$$

where ρ_w is the water density, κ_w is the bulk modulus. Based on the standard theories, (4) can be obtained as:

$$\frac{\rho_w}{C_w^{\,2}}\int_{V_w}\frac{\partial^2\phi}{\partial t^2}\delta\phi dV+\rho_w\int_{S_w}\dot{\mathbf{u}}\cdot\mathbf{n}\delta\phi dS+\rho_w\int_{V_w}\nabla\phi\cdot\delta\nabla\phi dV=0 \quad (6)$$

where V_w is the volume of water, S_w is the water boundary where normal velocity is prescribed. Under earthquake, the dynamic response of the water tank is coupled through compatibility of velocity potential and prescribed normal velocity at the fluid-structure interface. The system dynamic equations of the tank filled with water can be obtained [23]:

$$\begin{bmatrix}\boldsymbol{M}_{ss} & 0\\ 0 & -\boldsymbol{M}_{ww}\end{bmatrix}\begin{bmatrix}\ddot{\boldsymbol{U}}\\ \ddot{\boldsymbol{\Phi}}\end{bmatrix}+\begin{bmatrix}\boldsymbol{C}_{ss} & \boldsymbol{C}_{sw}\\ \boldsymbol{C}_{ws} & 0\end{bmatrix}\begin{bmatrix}\dot{\boldsymbol{U}}\\ \dot{\boldsymbol{\Phi}}\end{bmatrix}+\begin{bmatrix}\boldsymbol{K}_{ss} & 0\\ 0 & -\boldsymbol{K}_{ww}\end{bmatrix}\begin{bmatrix}\boldsymbol{U}\\ \boldsymbol{\Phi}\end{bmatrix}=\begin{bmatrix}-\boldsymbol{M}_{ss}\boldsymbol{I}\ddot{u}_g(t)\\ -\boldsymbol{C}_{ws}\boldsymbol{I}\dot{u}_g(t)\end{bmatrix} \quad (7)$$

In addition

$$\boldsymbol{M}_{ss}=\rho_s\int_{V_s}\boldsymbol{N}_s^T\boldsymbol{N}_s dV,\quad \boldsymbol{M}_{ww}=\frac{\rho_w}{C_w^2}\int_{V_w}\boldsymbol{N}_w^T\boldsymbol{N}_w dV$$
$$\boldsymbol{K}_{ss}=\rho_s\int_{V_s}\boldsymbol{N}_s^T\boldsymbol{D}_s^T\boldsymbol{N}_s dV,\quad \boldsymbol{K}_{ww}=\rho_w\int_{V_w}\boldsymbol{B}_w^T\boldsymbol{B}_w dV \quad (8)$$
$$\boldsymbol{C}_{sw}=\boldsymbol{C}_{ws}^T=-\rho_w\int_{V_w}\boldsymbol{N}_s^T\boldsymbol{n}\boldsymbol{N}_w dS,\ \boldsymbol{C}_{ss}=\alpha\boldsymbol{M}_{ss}+\beta\boldsymbol{K}_{ss}$$

where $\boldsymbol{N}_s$ and $\boldsymbol{N}_w$ are the standard isoparametric shape function matrices for shell and fluid elements respectively. ρ_s and V_s are the density and volume of the tank, $\boldsymbol{D}_s$ is the elastic matrix of shell elements, $\boldsymbol{M}_{ss}$ and $\boldsymbol{K}_{ss}$ are the mass and stiffness matrices for the tank, $\boldsymbol{M}_{ww}$ and $\boldsymbol{K}_{ww}$ are the mass and stiffness matrices for water. $\boldsymbol{I}$ is the column vector which has the same dimension of nodal relative displacement $\boldsymbol{U}$, $\boldsymbol{C}_{ws}$ and $\boldsymbol{C}_{sw}$ account for FSI between water and tank, $\boldsymbol{C}_{ss}$ is the Rayleigh damping matrix, in which α and β are the Rayleigh damping coefficients. The damping coefficients α, β and the matrix $\boldsymbol{B}_w$ in (5) are given by

$$\alpha=\frac{2\zeta\omega_1\omega_2}{\omega_1+\omega_2},\quad \beta=\frac{2\zeta}{\omega_1+\omega_2} \quad (9)$$

$$\boldsymbol{B}_w=\begin{bmatrix}\frac{\partial N_w^{(1)}}{\partial x} & \frac{\partial N_w^{(2)}}{\partial x} & \cdots & \frac{\partial N_w^{(n)}}{\partial x}\\ \frac{\partial N_w^{(1)}}{\partial y} & \frac{\partial N_w^{(2)}}{\partial y} & \cdots & \frac{\partial N_w^{(n)}}{\partial y}\end{bmatrix} \quad (10)$$

where ζ is the damping ratio of structure, ω_1 and ω_2 are the first and second natural frequencies of structure, n is the number of nodes per fluid element.

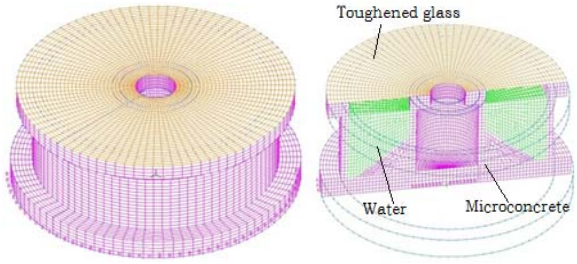

(a) (b)

Fig. 8 Numerical model of water tank (a) 3-D view, (b) Cross section

The experimental model is established based on ADINA. The model base and the tank walls are modeled using 3D solid finite elements, the toughened glass is modeled using shell finite element and the water is modeled using 3D PBFE. The material parameters are the same with experiment shown in Table I. The numerical model is shown in Fig. 8.

B. Modal Analysis and Comparison

Considering the symmetry of structure, the repeated modes are ignored. The first four sloshing frequencies and the sloshing modes are shown in Fig. 9. The frequencies are compared with the experimental results, and the errors are listed in Table IV. The errors of 1st, 2nd and 4th sloshing frequencies are all less than 1%. Although the error of 3rd sloshing frequency is larger than other three, 6.15% error is acceptable. Through the comparison, the reasonableness of numerical analysis and the accuracy of experimental results are verified.

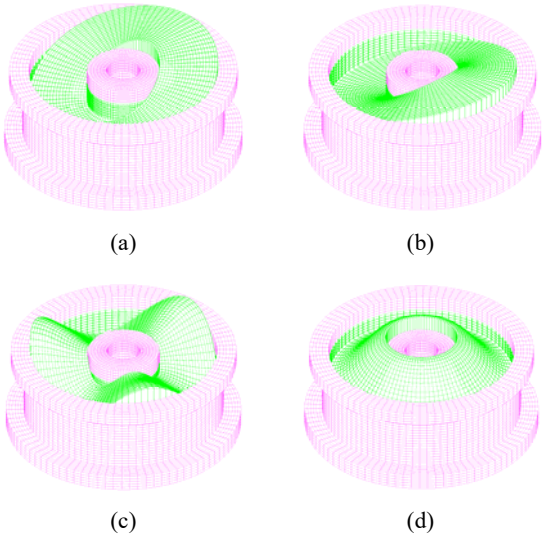

(a) (b) (c) (d)

Fig. 9 First four sloshing modes (a) 1st sloshing frequency 0.4926 Hz, (b) 2nd sloshing frequency 0.8399 Hz, (c) 3rd sloshing frequency 1.0631 Hz, (d) 4th sloshing frequency 1.2085 Hz

C. Time History Analysis and Comparison

In this part, the reasonableness of numerical analysis is verified in time history analysis. The three-direction acceleration time histories are used as inputs at the foundation

of model and the time history curves are shown in Fig. 4 (b). The durations of inputs are 6.142 s, and the duration of strong motion is about 3.50 s. Considering the free sloshing of water, the calculation time is extended to 10 s.

TABLE IV
FIRST FOUR SLOSHING FREQUENCIES

Sloshing modes	Average value (Hz)	Numerical analysis (Hz)	Errors (%)
1	0.4938	0.4926	-0.24
2	0.8404	0.8399	-0.06
3	1.0015	1.0631	+6.15
4	1.2188	1.2085	-0.85

Under the three-direction seismic loadings, the water is rotating along the walls of tank. The numerical results of vertical sloshing displacement are shown in Fig. 10. It can be seen that the maximum vertical displacement appears at the junction of water and inner tank wall. Moreover, the maximum vertical displacement not only appears in X axis or Y axis but also in other direction shown as Fig. 10 (a). The reason may be that the height of inner wall is lower than outer wall and the sloshing response is stronger near the inner wall. After the seismic loadings, the water is sloshing continuously and the attention is small.

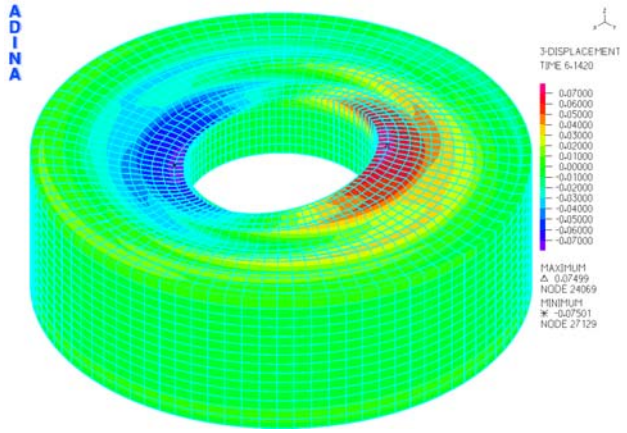

(a)

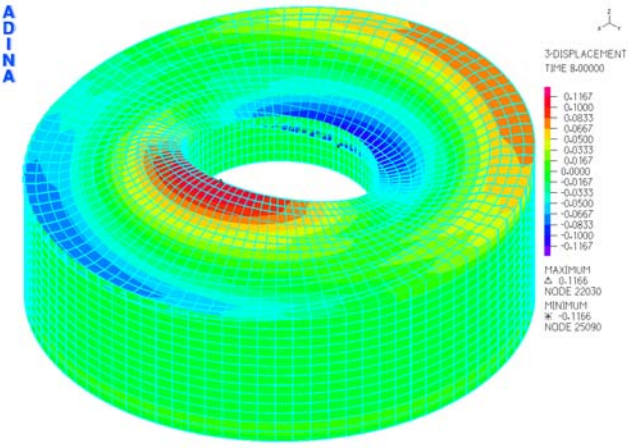

(b)

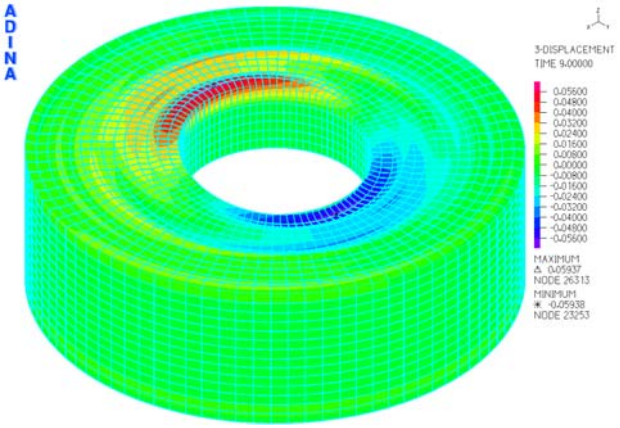

(c)

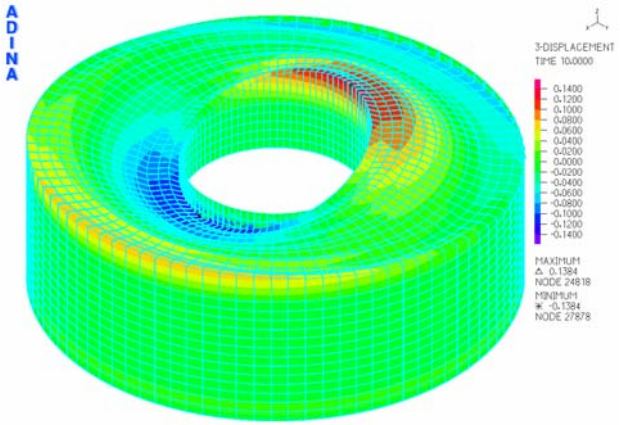

(d)

Fig. 10 Numerical results of vertical sloshing displacement (a) Vertical sloshing displacement at 6.142 s, (b) Vertical sloshing displacement at 8.000 s, (c) Vertical sloshing displacement at 9.000 s, (d) Vertical sloshing displacement at 10.000 s

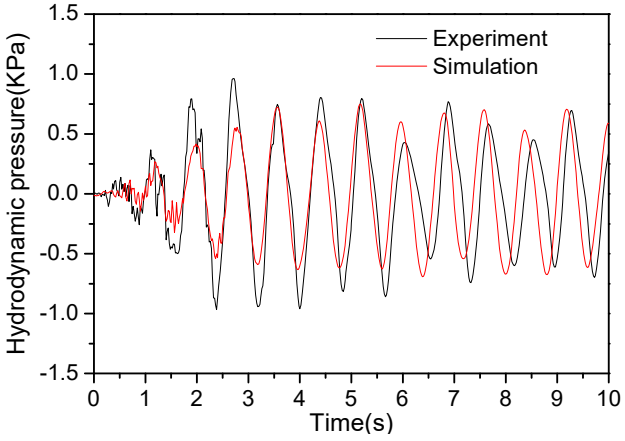

(a)

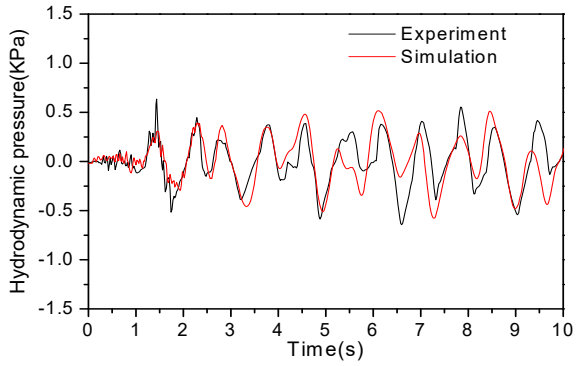

(b)

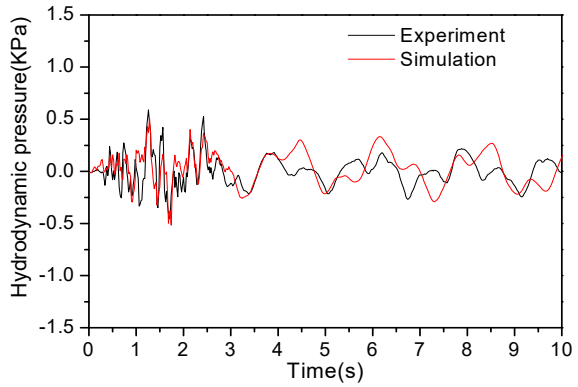

(c)

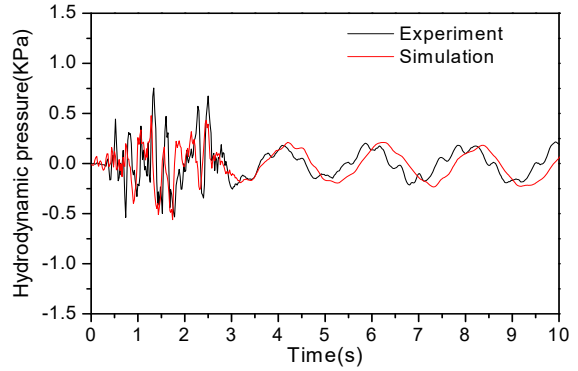

(d)

Fig. 11 The hydrodynamic pressure under three-direction seismic loadings (a) No.8 PWPS, (b) No.9 PWPS, (c) No.10 PWPS, (d) No. 12 PWPS

The hydrodynamic pressure results of numerical model are compared with those of the experiment. Four reference points at the outer wall, inner wall, and bottom are chosen for comparison and the results are shown in Fig. 11. The locations of PWPS are shown in Fig. 3.

Fig. 11 (a) shows the hydrodynamic pressure time history of No. 8 PWPS. The shapes of two curves are in good agreement generally. At the duration of seismic loadings (0-6.142 s), the curve of simulation has the smaller peaks than experimental one. In the stage of free sloshing, the peaks of two curves are close. But, the corresponding times of peaks are not same and have some deviations.

Fig. 11 (b) shows the hydrodynamic pressure time history of No. 9 PWPS. The simulation data agree well with the experimental results in the shape of curve and the peaks. However, the experimental results are larger obviously at certain time points.

Fig. 11 (c) shows the hydrodynamic pressure time history of No. 10 PWPS. The two curves do not have good agreement, especially after the strong motion. But, the peaks of two curves are close in the first 3 s.

Fig. 11 (d) shows the hydrodynamic pressure time history of No. 12 PWPS. The trends of two curves are similar to Fig. 11 (a). The curve of simulation has the smaller peaks in the duration of strong motion. Moreover, the peaks of two curves are close after 3.5 s.

The four PWPS are located at outer wall, inner wall, the bottom, the junction of wall and bottom separately. So, the comparison results can verify the reasonableness of numerical analysis. The simulation data in Figs. 11 (a), (b) and (d) agree with the experimental results in general. No. 8 and No. 9 PWPS are close to the free liquid surface, and No. 12 PWPS is at the middle of inclined bottom. So, the sloshing response of the three reference points are simple and the curves agree well. The simulate data of No. 10 PWPS fit poorly with experimental results. After the water hits the inclined bottom, it would flow to the nearby tank wall and hit the PWPS on it. This may make the sloshing response of water complicated, especially at the junction of tank wall and inclined bottom. Therefore, the numerical analysis could not simulate the sloshing response precisely at that time. That is why the comparison result of No. 10 PWPS is not as accurate as the other three PWPS.

In general, the formulation of PBFE can be used to simulate the sloshing response of liquid, and the accuracy is acceptable. On the other hand, the hydrodynamic pressure is small, and the researchers need to pay more attention to the safety of water tank. But, the seismic response of nuclear island building with water tank should be taken seriously.

IV. Conclusion

A shaking table test on 1/16 scaled model was designed and was done in this study for the irregular annular cylindrical water tank of nuclear island building. PWPS and cameras were used to record the hydrodynamic pressure time histories and the attenuation data of wave height. The sloshing frequencies are recognized by FFT of hydrodynamic pressure time histories and the sloshing damping ratio are calculated using logarithmic decrement method. A numerical model is established based on ADINA. Then, modal analysis and time history analysis are done, and the numerical results are compared with experimental data. The following conclusions can be drawn.

(1) The measuring methods of the water responses mentioned in this paper can be used to recognize sloshing frequency and damping ratio. Moreover, these methods are simpler and more practicable than using laser displacement sensor.
(2) The sloshing damping ratio of irregular annular cylindrical water is 0.5138%, and it has a good agreement with the

suggestion of regular tanks. It implies that the sloshing damping ratio could not be influenced obviously by the shape of water tank.

(3) The formulation of PBFE is suitable for modal analysis and time history analysis. The accuracy of numerical results is acceptable.

ACKNOWLEDGMENT

This research is supported by National Science and Technology Major Project (2013ZX06002001-9) and Natural Science Foundation of China (51421005).

REFERENCES

[1] T.L. Schulz, "Westinghouse AP1000 advanced passive plant," Nuclear Engineering and Design, vol. 236, no. 14–16, 1547-1557, 2006.
[2] C. Zhao, J. Chen, "Dynamic characteristics of AP1000 shield building for various water levels and air intakes considering fluid-structure interaction," Progress in Nuclear Energy, vol. 70, no.3, 176-187, 2014.
[3] C. Zhao, J. Chen, Q. Xu, "Dynamic analysis of AP1000 shield building for various elevations and shapes of air intakes considering FSI effect subjected to seismic loading," Progress in Nuclear Energy, vol. 74, no.3, 44-52, 2014.
[4] C. Zhao, J. Chen, and Q. Xu, "FSI effects and seismic performance evaluation of water storage tank of AP1000 subjected to earthquake loading" Nuclear Engineering and Design, vol. 280, 372-388, 2014.
[5] Q. Xu, J. Chen, C. Zhang, J. Li, C. Zhao, "Dynamic analysis of AP1000 shield building considering fluid and structure interaction effects," Nuclear Engineering and Technology, vol. 48, no. 1, 246-258, 2016.
[6] D. Lu, Y. Liu, and X. Zeng, "Experimental and numerical study of dynamic response of elevated water tank of AP1000 PCCWST considering FSI effect," Annals of Nuclear Energy, vol. 81, 73-83, 2015.
[7] Y. Liu, D. Lu, J. Dang, "Equivalent mechanical model for structural dynamic analysis of elevated tank like AP1000 PCCWST," Annals of Nuclear Energy, vol. 85, 1175-1183, 2015.
[8] X. Zeng, D. Lu, J. Dang, and Y. Liu "Research on sloshing characteristics in passive cooling storage tank of AP1000 under long-period earthquake," Nuclear Power Engineering, vol.36, no. 5, 91-95, 2015.
[9] D. Lu, "Sloshing response of the free surface in the main vessel of CEFR excited by 3 sine waves," Chinese Journal of Nuclear Science and Engineering, vol. 23, no. 4, 306-310, 2003.
[10] W. Wang, H. Xia, and J. Li, "Experimental investigation of nonlinear liquid sloshing in a hemispherical container," Journal of Tsinghua University (Science and Technology), vol. 48, no. 11, 32-36, 2008.
[11] H. Takahara, K. Kimura, "Frequency response of sloshing in an annular cylindrical tank subjected to pitching excitation," Journal of Sound and Vibration, vol. 331, 3199-3212, 2012.
[12] J. Wang, J. Lu, "Study on the sloshing simulation system of cargo tanks on ships," Journal of Zhejiang Ocean University (Natural Science), vol. 33, no. 3, 223-226, 2014.
[13] S. Li, F. Gao, Y.R. Yang, and C.G. Fan, "Finite element modal analysis and dynamic experimental for liquid sloshing," Nuclear Power Engineering, vol. 28, no. 4, 54-57, 2007.
[14] D.D. Kana, "Status and research needs for prediction of seismic response in liquid containers," Nuclear Engineering and Design, vol. 69, no. 2, 205-221, 1982.
[15] G.W. Housner, "Dynamic pressure on accelerated fluid containers," Bulletin of the seismological society of American, vol. 44, no. 1, 15-35, 1957.
[16] G.W. Housner, "The dynamic behavior of liquid in moving containers," Bulletin of the seismological society of American, vol. 53, no. 2, 381-387, 1963.
[17] ASCE 4-98, "Seismic analysis of safety-related nuclear structures and commentary," American society of civil engineers.
[18] ACI 350.3-06, "Seismic design of liquid-containing concrete structures and commentary," American Concrete Institute.
[19] The Steel Construction Institute, "Fluid structure interaction effects on and dynamic response of pressure vessels and tanks subjected to dynamic loading," RR527, The Steel Construction Institute, the United Kingdom, 2007.
[20] ADINA R&D, "Theory and modeling guide," Rep. ARD 10-7, ADINA R&D, Watertown, MA, 2010.
[21] K. Wei, W. Yuan, and N. Bouaanani, "Experimental and numerical assessment of the three-dimensional modal dynamic response of bridge pile foundations submerged in water," Journal of Bridge Engineering, vol. 18, no. 10, 1032-1041, 2013.
[22] N. Bouaanani, F.Y. Lu, "Assessment of potential-based fluid finite element for seismic analysis of dam-reservoir systems," Computers & Structures, vol. 87, no. 3, 206-224, 2009.
[23] L.G. Olson, K.J. Bathe, "Analysis of fluid–structure interactions: a direct symmetric coupled formulation based on the fluid velocity potential," Computers & Structures, vol. 21, no. 1-2, 21–32, 1985.

X. J. Li was born in Hunan, China in 1965. Following a B.S. in 1984 from the department of civil engineering, Hunan University, China, Li went to the Institute of Engineering Mechanics (IEM), CEA, China for an S.M. (1987) and Ph.D (1993), all in earthquake engineering.

Earthquake Administration as a postdoctor from 1993-1995, and as a full professor from 1996-2004, 2010-present. He worked at Cardiff Institute, Wales University, UK as a visiting professor from 1997-1998, and at Institute of Engineering Mechanics, China Earthquake Administration as a full professor from 2004-2010. His research covers research fields of seismology, earthquake engineering, and disaster prevention and mitigation.

Professor Li is a Member of Executive Committee of International Society of Lifeline and Infrastructure Earthquake Engineering a steering committee member and management board member of Consortium of Asia-Pacific Region Global Earthquake and Volcanic Eruption Risk Management (GEVER), an executive director of the Seismological Society of China, the editor in chief of Recent Developments in World Seismology, the associate editor in chief of the Translated World Seismology, the associate editor in chief of the Technology for Earthquake Disaster Prevention.